

MEASUREMENT OF $\alpha\alpha$ AND αp ELASTIC SCATTERING AT THE CERN ISR

W. Bell¹⁾, K. Braune²⁾, G. Claesson³⁾, D. Drijard¹⁾, M.A. Faessler²⁾,
H.G. Fischer¹⁾, H. Frehse¹⁾, R.W. Frey⁴⁾, S. Garpman³⁾, W. Geist¹⁾,
P.C. Gugelot⁶⁾, P. Hanke¹⁾, M. Heiden⁵⁾, P.G. Innocenti¹⁾, T.J. Ketel²⁾,
E.E. Kluge⁵⁾, G. Mornacchi¹⁾, T. Nakada⁵⁾, I. Otterlund³⁾, B. Povh²⁾,
A. Putzer⁵⁾, E. Stenlund³⁾, T.J.M. Symons⁷⁾, R. Szwed^{2,8)}, O. Ullaland¹⁾,
and Th. Walcher²⁾

ABSTRACT

Differential cross-sections for $\alpha\alpha$ and αp scattering have been measured at $\sqrt{s} = 125$ and 88 GeV, respectively, in the t range from -0.2 to -0.8 (GeV/c)² using the Split-Field Magnet detector at the CERN Intersecting Storage Rings. Comparison with theoretical calculations using the Glauber model confirms the importance of including inelastic shadowing effects in very high energy nucleus-nucleus elastic scattering.

(Submitted to Physics Letters)

-
- 1) CERN, Geneva, Switzerland.
 - 2) Max-Planck Institut für Kernphysik, Heidelberg, Fed. Rep. Germany.
 - 3) Division of Cosmic and Subatomic Physics, University of Lund, Sweden.
 - 4) Physikalisches Institut der Univ. Heidelberg, Fed. Rep. Germany.
 - 5) Institut für Hochenergiephysik, Heidelberg, Fed. Rep. Germany.
 - 6) Physics Department, University of Virginia, Charlottesville, Va., USA.
 - 7) Nuclear Science Div., Lawrence Berkeley Lab., Berkeley, Calif., USA.
 - 8) On leave from the Inst. of Experimental Physics, Warsaw, Poland.

1. INTRODUCTION: The success of the Glauber model in describing hadron-nucleus and nucleus-nucleus elastic scattering at high energy has demonstrated that the main features of the differential cross-sections can be explained by the interference between single and multiple scattering terms [1]. However, it has been speculated that at very high energy it is necessary to modify the Glauber formulae by the inclusion of terms arising from coherent excitation of intermediate inelastic states [2]. Such corrections provide an interesting application for techniques of Reggeon field theory, as the corresponding amplitude can be related to the triple-pomeron coupling [3]. Experimentally, it is claimed that the effects have been observed in pd and dd scattering at the CERN Intersecting Storage Rings (ISR) [4] and in p α scattering at FNAL [5]. There are, however, still unresolved discrepancies between these and other experiments with respect to the size of the effect [7,6]. The successful acceleration and storage of α particles in the ISR has allowed a further test of these effects at the highest centre-of-mass energies yet studied for proton-nucleus and nucleus-nucleus collisions.

We have measured the differential elastic scattering cross-section as a function of four-momentum transfer t , using the Split Field Magnet (SFM) detector. The t range of our measurements [$0.2 < |t| < 0.8$ (GeV/c)²] is complementary to the one of the CERN-MIT-Naples-Pisa-Stony Brook Collaboration [8] [$0.05 < |t| < 0.3$ (GeV/c)²], which took data simultaneously with us at another intersection.

2. THE SET-UP: The data were obtained under two separate beam conditions. In the first run, two beams of α particles of 62.9 GeV/c were circulated ($\sqrt{s} = 124.6$ GeV); in the second run, a 62.9 GeV/c α beam and a 31.5 GeV/c proton beam were stored ($\sqrt{s} = 88.0$ GeV). The total integrated luminosity was 2.3×10^{33} cm⁻² (αp) and 1.9×10^{33} cm⁻² ($\alpha\alpha$). A sketch of the experimental arrangement is shown in fig. 1. The trigger for an elastic event required a coincidence between the large scintillator arrays T1 and T2, and also the presence of two tracks passing through the multiwire proportional chambers (MWPCs) surrounding the beam pipe in the SFM compensator magnets. These tracks were defined by a coincidence between three horizontal wire planes (see fig. 1b). Approximate

collinearity of the three coordinates was required by coincidences between wire groups in different horizontal wire planes. Each group consisted of 32 adjacent wires. The trigger logic was built using MBNIM electronics developed at CERN [9]. A further coincidence matrix was set up to ensure collinearity between the two tracks.

3. ANALYSIS: The data obtained were analysed using the following procedure. Most of the events recorded by the trigger contained not α particles but rather fast protons from α particle break-up. The great majority of these events could be rejected by cuts on the pulse height from the scintillators. This filter did not, however, remove ^3He fragments or the tail of the proton energy loss distribution. The remaining events were then reconstructed using the wire information. The t value was determined by measuring the displacement of the track with respect to the undisturbed beam. Since the beam momentum varies as a function of position within the beam stack, the two tracks were first considered independently in order to obtain the vertex position and thence the momenta of the two scattered beam particles. A constrained fit was then made, including the correct elastic scattering kinematics, in order to determine the momentum transfer. It should be emphasized that although the magnetic field is not included explicitly in this procedure, its effect is of course very strong in the rejection of tracks that are collinear but do not have the correct momenta. In particular, protons ($p/Z = 15 \text{ GeV}/c$) and ^3He nuclei ($p/Z = 22.5 \text{ GeV}/c$) are rejected very effectively by the χ^2 test. By means of Monte Carlo calculations it was found that even events with a single unobserved π^0 would be rejected at the 95% level.

4. ACCEPTANCE: The most important corrections are those due to geometrical acceptance and reaction losses in the trigger telescopes.

The geometrical cut-off at low angles, caused by the vacuum pipe, is at 7 mrad, which corresponds to $|t| = 0.2 (\text{GeV}/c)^2$ for an incoming momentum of 62 GeV/c. For the present data, the cut-off at high t values is only due to the limited

amount of beam time. The acceptance of the apparatus has been calculated using events generated by a Monte Carlo procedure and reconstructed by the same analysis program as real events.

The reaction probability in the chamber material, the trigger scintillators, and the beam pipe is very large at low t , being of the order of 50% for each α track. This introduces a considerable uncertainty in the measured cross-sections for $|t|$ smaller than 0.4 (GeV/c)^2 . The absorption loss of tracks was calculated by Monte Carlo procedures and was cross-checked by two independent methods. First, the measured pp elastic scattering distribution was compared with existing measurements and, secondly, the azimuthal (ϕ) distributions (at fixed t) of the $\alpha\alpha$ and αp data were examined and compared with the expectations from the reaction losses. The results of these checks are in reasonable agreement, but the corrections to the lowest $|t|$ points are large and provide the biggest contribution to the errors. The uncertainty in the normalization of the cross-section due to the error in the luminosity measurement is estimated to be of the order of 10%.

5. RESULTS: The measured distributions are given in fig. 2 and in table 1. Our result for the αp cross-section is shown in fig. 2a. Unfortunately, the lower t value is right at the first diffraction minimum. The data are compared with a recent calculation of Proriot et al. [10] and with the data from the gas jet experiment at FNAL [5]. The dotted line was calculated in the Glauber model, using the following input parameters: for the p-nucleon amplitude, a total cross-section of 41.8 mb and a slope of 12.98 GeV^{-2} ; and for the nuclear wave function, the Fourier transform $S(q, q')$ of the nucleon density [11]. The solid line represents a calculation where an inelastic shadow correction was introduced into the double scattering term. The mass spectrum of the intermediate excited state was separated, following Alberi [3], into two regions: a low-mass region dominated by resonance production, and a high-mass region dominated by the triple Regge interaction.

The result for the $\alpha\alpha$ differential cross-section is shown in fig. 2b (together with the result of an experiment done at Saclay [12]). Here we make a comparison with calculations done by Alberi et al. [13]. Again, the dotted line is a calculation in the pure Glauber model [with: $\sigma_{\text{tot}}(\text{NN}) = 40.2 \text{ mb}$; slope $b = d \ln(d\sigma/dt)/dt = 12.2 (\text{GeV}/c)^{-2}$ at small $|t| < 0.15 (\text{GeV}/c)^2$; real to imaginary part of the NN amplitude $\rho = 0$; and a single Gaussian α form factor with mean square radius $\langle R^2 \rangle^{1/2} = 1.66 \text{ fm}$]. The second curve shows the effect of introducing inelastic intermediate states. In this case the correction has to be applied not only to the double scattering term but also to higher-order multiple scattering ones. The effect is considerably larger than in αp , since the multiple scattering terms have a higher weight. It has to be appreciated, however, that at present there is still some uncertainty concerning the correct wave function to be used for the α particle.

Whilst the precision of our αp data is not sufficient for deciding whether the inelastic shadow correction to the Glauber calculation is needed or not, it is seen that in the $\alpha\alpha$ cross-section this correction, which is very large in our t range, is needed, even taking into account the systematic and statistical uncertainty of the data.

Acknowledgements: We wish to thank G. Goggi for helpful advice at the planning stage of the experiment, F. Bourgeois for supplying us with the necessary MBNIM logic modules, R. Messerli for programming help, W. Heibel and G. Ochmann for help during the setting up of the trigger, and G. Alberi and J. Proriol for providing their calculations and for instructive discussions.

REFERENCES

- [1] R.J. Glauber, *in* Lectures in Theoretical Physics (eds. W.C. Brittin and L.G. Dunham) (Interscience Publ., NY, 1959), Vol. 1, p. 315.
V. Franco and R.J. Glauber, Phys. Rev. 142 (1966) 1195.
R.J. Glauber, Proc. 2nd Int. Conf. on High-Energy Physics and Nuclear Structure, Rehovoth, 1967 (ed. G. Alexander) (North Holland Publ. Company, Amsterdam, 1967), p. 311.
- [2] E.S. Abers et al., Nuovo Cimento 42A (1966) 365.
V.N. Gribov, Sov. Phys. JETP 29 (1969) 483.
J. Pumplin and M. Ross, Phys. Rev. Lett. 21 (1968) 1778.
G. Alberi and L. Bertocchi, Nuovo Cimento 61A (1969) 201.
D.R. Harrington, Phys. Rev. D 1 (1970) 260.
C. Quigg and L.L. Wang, Phys. Lett. 42B (1973) 314.
- [3] G. Alberi and G. Goggi, Phys. Reports 74 (1) (1981) 1.
- [4] G. Goggi et al., Phys. Lett. 77B (1978) 428.
G. Goggi et al., Phys. Lett. 77B (1978) 433.
G. Goggi et al., Nucl. Phys. B149 (1979) 381.
- [5] A. Bujak et al., Phys. Rev. D 23 (1981) 1895.
- [6] G. Warren et al., Imperial College (London) preprint IC/HENP 81-5 (1981).
- [7] J.P. Burq et al., Nucl. Phys. B187 (1981) 205.
- [8] M. Ambrosio et al., preprint CERN-EP/81-117, submitted to Phys. Lett. B.
- [9] A. Beer et al., Nucl. Instrum. Methods 160 (1979) 217.
F. Bourgeois, CERN-EF/79-3, paper presented at the Nuclear Science Symposium, San Francisco, 1979.
- [10] J. Proriot, S. Maury and B. Jargeaix, Phys. Lett. 110B (1982) 95.
- [11] J. Proriot et al., On the introduction of a Fourier transform in the Glauber method for the study of hadron-helium elastic scattering, Univ. de Clermont II preprint PCCF RI 82/01 (1982).

- [12] J. Berger et al., Nucl. Phys. A338 (1980) 421.
- [13] G. Alberi, private communication.

Table 1

Measured elastic differential cross-sections

$-t \left[\frac{\text{GeV}}{c} \right]^2$	$\left. \frac{d\sigma}{dt} \right _{\alpha\alpha} \left[\frac{10^{-30} \text{ cm}^2 \text{ c}^2}{\text{GeV}^2} \right]$	$\left. \frac{d\sigma}{dt} \right _{\alpha p} \left[\frac{10^{-30} \text{ cm}^2 \text{ c}^2}{\text{GeV}^2} \right]$
0.2375		50.207 ± 9.431
0.2625	277.289 ± 31.945	112.301 ± 8.687
0.2875	160.493 ± 19.756	160.795 ± 9.380
0.3125	71.272 ± 11.453	191.910 ± 9.163
0.3375	30.040 ± 6.341	181.674 ± 8.432
0.3625	15.065 ± 3.561	139.461 ± 7.073
0.3875	4.768 ± 1.496	120.407 ± 7.080
0.4125	5.605 ± 1.516	79.939 ± 5.675
0.4375	4.828 ± 1.210	62.460 ± 4.825
0.4625	5.711 ± 1.230	38.884 ± 3.191
0.4875	7.574 ± 1.416	32.376 ± 2.869
0.5125	5.102 ± 1.071	24.180 ± 2.416
0.5375	5.946 ± 1.120	17.969 ± 1.915
0.5625	3.807 ± 0.868	9.433 ± 1.356
0.5875	3.718 ± 0.851	6.483 ± 1.169
0.6125	2.996 ± 0.731	5.237 ± 1.018
0.6375	2.526 ± 0.652	5.137 ± 1.153
0.6625	0.503 ± 0.281	2.990 ± 0.903
0.6875	1.252 ± 0.456	1.969 ± 0.702
0.7125	0.498 ± 0.278	3.392 ± 1.394
0.7375	0.757 ± 0.362	
0.7625	0.198 ± 0.175	
0.7875	0.0	
0.8125	0.097 ± 0.121	
0.8375	0.097 ± 0.121	

Figure captions

- Fig. 1 : The experimental set-up at the Split-Field Magnet. a) Horizontal view, showing main magnet (SFM) and the two compensator magnets (C1, C2), multiwire proportional chambers labelled 313, ... , 417, and the scintillator hodoscopes T1 and T2. b) Vertical view of the chambers, hodoscopes, and the vacuum tube. The 32-wire groups are indicated.
- Fig. 2 : Differential α_p (a) and α_α (b) elastic cross-section, compared with FNAL [5] and Saclay [12] data. The final efficiencies (geometrical acceptance times the transmission through absorbers) are also shown; the horizontal error bars indicate the resolution in t . The data are compared with Glauber model calculations by Proriol et al. [10] and Alberi et al. [13] with and without intermediate inelastic state (IIS) corrections.

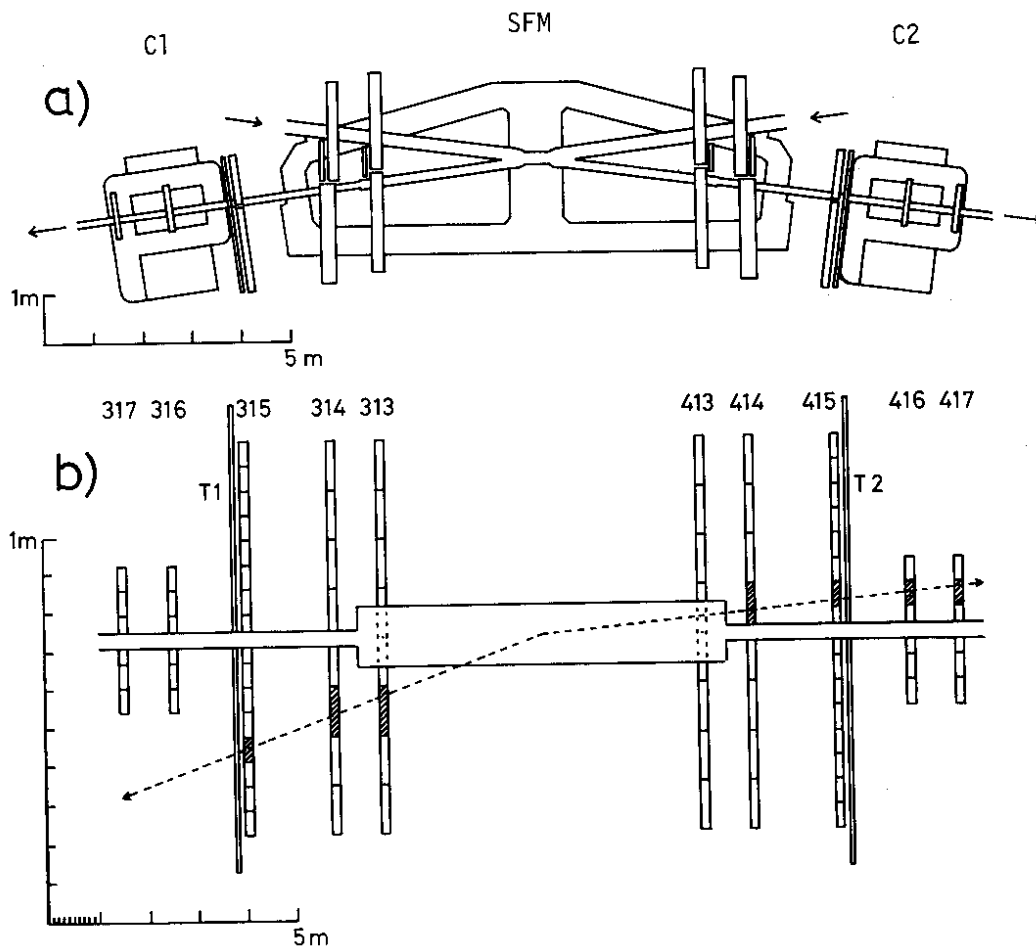


Fig. 1

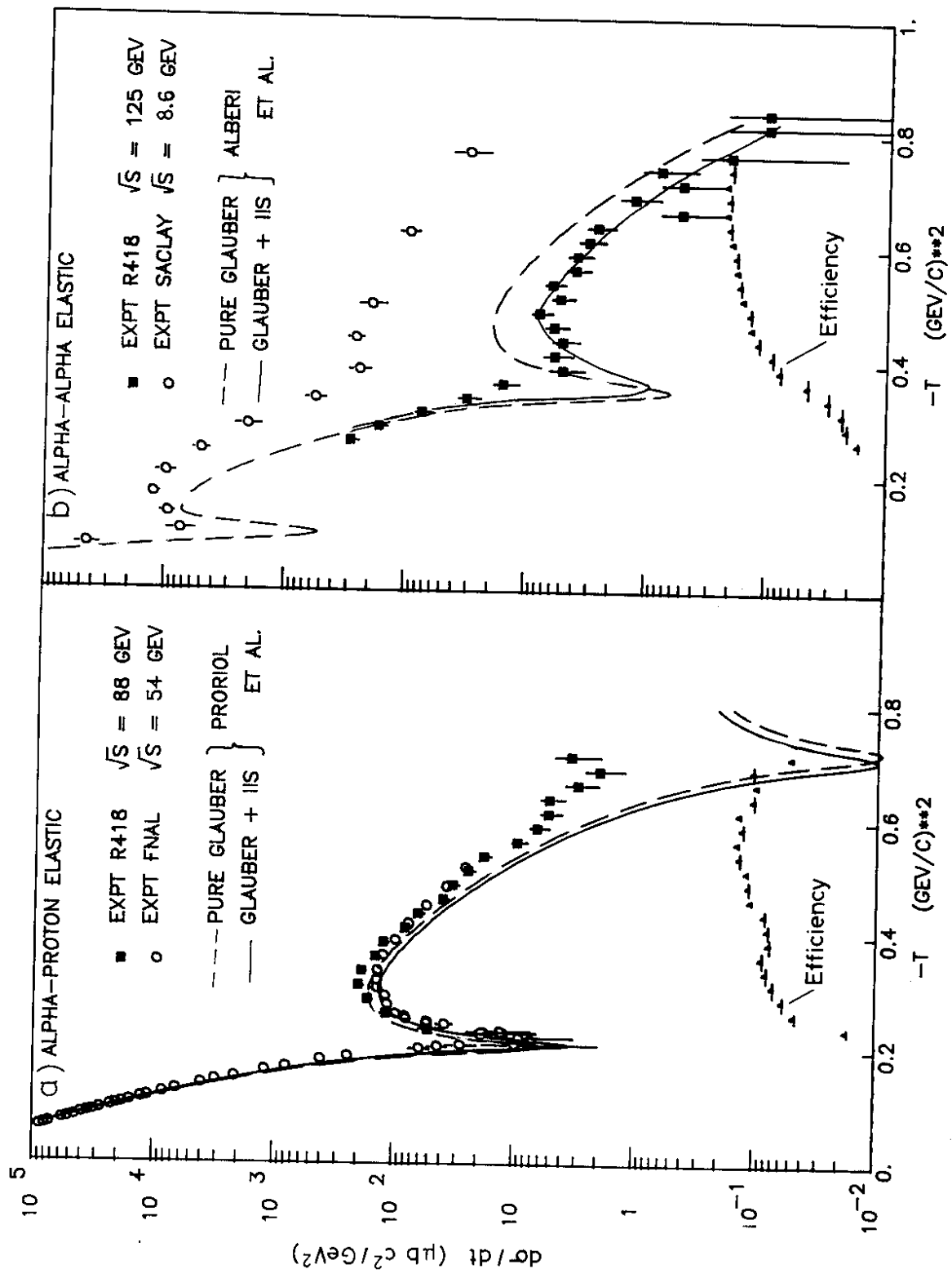


Fig. 2